Correlation of intraprostatic tumor extent with ^{68}Ga-PSMA distribution in patients with prostate cancer

Kambiz Rahbar[1], Matthias Weckesser[1], Sebastian Huss[2], Axel Semjonow[3], Hans-Jörg Breyholz[1], Andres J. Schrader[3], Michael Schäfers[1,4,5], and Martin Bögemann[3]

1. Department of Nuclear Medicine, University Hospital Muenster, Muenster, Germany
2. Gerhard Domagk Institute of Pathology, University Hospital Muenster, Muenster, Germany
3. Department for Urology, Prostate Center, University Hospital Muenster, Muenster, Germany
4. European Institute for Molecular Imaging, University of Muenster, Muenster, Germany
5. Cells-in-Motion, Center of Excellence, University of Muenster, Muenster, Germany

Running Title: Intraprostatic PCa and PSMA-PET/CT

Keywords: PSMA-PET/CT, Prostate Cancer, pilot study, Prostatectomy.

Word count: 3706

Corresponding Author:

Dr. Kambiz Rahbar

Department of Nuclear Medicine

University Hospital Muenster

Albert-Schweitzer-Campus 1

48149 Muenster, Germany

Phone: +49-251-83-47362

Fax: +49-251-83-47363

E-mail: rahbar@uni-muenster.de

Abstract

Purpose: We evaluated the diagnostic value and accuracy of prostate specific membrane antigen (PSMA) positron emission tomography (PET) for the intraprostatic delineation of prostate cancer prior to prostatectomy.

Methods: We identified a total of six patients with biopsy proven high risk prostate cancer, who were referred to ^{68}Ga-PSMA-PET/CT prior to radical prostatectomy to rule out metastases. After prostatectomy, a histology map of the prostate was reconstructed. The histological extension and Gleason Score of each segment of the prostate were compared with PSMA-PET images, resliced to the histological axis. Sensitivity, specificity, positive predictive value, negative predictive value, positive and negative likelihood ratios were calculated. Standard uptake value of each segment was measured and median values were compared.

Results: 112/132 segments were eligible for analysis. The correlation of histological results with PSMA-PET images showed a specificity and sensitivity of 92%, respectively. The positive and negative likelihood ratio and the positive and negative predictive value for PSMA-PET detecting prostate cancer were 11.5, 0.09, 96% and 85%, respectively. The median maximum standard uptake value of true positive prostate segments was significantly higher than in true negative segments (11.0±7.8 vs. 2.7±0.9, p<0.001) and a cutoff of 4 revealed a sensitivity and specificity of and 86.5% and an accuracy of 87.5%.

Conclusions: These preliminary results show that the intraprostatic localization and extent of prostate cancer may be estimated by PSMA-PET. This imaging method may be helpful for identifying target lesions prior to prostate biopsy and may support decision-making prior to focal or radical prostate cancer therapy.

Introduction

Prostate cancer (PCa) is the most common cancer in men. Within the USA an estimated 26% of cancer cases are expected to be PCa in 2015 *(1)*. PSA-based screening leads to a significant proportion of overdiagnosis *(2)* and consequently overtreatment *(3)*. Overtreatment is partly caused by unknown true tumor extent prior to prostate biopsy as well as the planning of a definitive tumor therapy.

Prostate Specific Membrane Antigen (PSMA) is a transmembrane protein *(4)*. It is expressed in prostate epithelial cells with increased expression in PCa cells. The expression levels increase with PCa progression *(5, 6)*. PSMA is expressed in some normal tissues (e.g. small intestine, renal tubules or salivary glands) *(7)* but in PCa expression levels are 100-1000 fold higher *(8)*. Recently developed ^{68}Ga-labelled PSMA-ligands showed to be of high specificity and sensitivity for the detection of recurrent PCa and metastatic disease *(9)*.

PSMA-based imaging may have the potential to exactly charactarize the extent of intraprostatic disease and could therefore be a useful tool to identify and define malignant lesions prior to prostate biopsy, and finally to help tailoring an optimal definitive therapy for each patient. Therefore, the aim of this proof of concept study was to analyze the performance of ^{68}Ga-labelled PSMA-PET/CT for the prediction of the true extent of PCa within the prostate and seminal vesicles.

Materials and Methods

Patient population

Between May 2014 and August 2015 six patients (age, 65±8.2 years, range 56-73) with biopsy proven PCa who had a PSMA-PET/CT 3-32 days before radical prostatectomy (RPE) due to high risk of extraprostatic manifestation of PCa were identified. Transrectal ultrasound (TRUS)-guided prostate biopsy (pBx) had been performed in all patients with 6 to 14 cores. Local and external reference pathology institutions performed histological analysis and Gleason score grading. PSMA-PET/CT imaging was performed to rule out metastatic PCa. The indication for PSMA imaging was appointed by an interdisciplinary tumor board. All patients signed an informed consent form before PET/CT imaging. In two patients metastases were found (a single bone metastasis in one patient and nodal involvement in another patient). Due to increasing evidence that RPE in spite of nodal tumor involvement or in patients with no more than three bone lesions may transfer into delayed progression, delay of castration resistant prostate cancer and may even lead to prolonged survival outcomes *(10, 11)*. After a very thorough clarification of the available data the possibility of RPE was offered to these patients. Both patients consented to having the RPE performed. The institutional review board approved this retrospective study and the requirement to obtain informed consent was waived.

Patient preparation and PSMA-PET/CT

Whole body PET/CT was performed 65.1±7.0 minutes after injection of 161±19.8 MBq (range, 131-193 MBq) ^{68}Ga-PSMA-HBED-CC (DKFZ-Ga-PSMA-11) *(12)*. Patients were

asked to void immediately before scanning. The scans were obtained using a high resolution hybrid PET/CT system (Biograph mCT with a 128 Slice CT; Siemens Medical Solutions, Knoxville, TS). Low-dose CT of the entire area covered by PET (from skull to the mid thigh level) was performed for attenuation correction. After completion of the CT scan, PET data were acquired for three minutes per bed position. PET images were reconstructed using the standard manufacturer-supplied software (PET resolution of 3 mm).

Image analysis

Clinical analysis of the images prior to RPE was performed by 2 board certified radiologists and nuclear medicine physicians. Standard uptake value (SUVmax) was measured within each prostate segment after reangulation of the images correlative to histology slices of the prostate from base to apex axial to the course of the urethra. Correlative analysis of the PSMA-images and the postoperative histology maps was performed by a board certified urologist, a board certified nuclear medicine physician and a board certified pathologist according to true positive, true negative, false positive and false negative segments of the prostate gland.

Pathological evaluation

RPE was performed in all six patients. The prostate specimens were processed and evaluated according to the local standard operation procedures of the Institute of Pathology *(13)*. After macroscopic examination the prostate and the seminal vesicles were fixed in 10% neutral buffered 4% formalin solution (approx. 4% formaldehyde). The gland was prepared for histology by a modified version of the technique introduced by

the Association of Clinical Pathologists *(14)*. After removal of the apex and the base of the prostate the gland was cut transversally into slices of 5 mm thickness.

Finally, the slices were separated in right and left halves and front and back sections. The complete slices of the specimen were embedded in paraffin and the blocks were cut into 4-µm slices. Hematoxylin and eosin staining and microscopic examination were performed. Gleason score *(15)* and staging according to the Union international contre le cancer (UICC) and tumor-lymph node-metastasis (TNM) staging system were determined *(16)*.

Topographical analysis

The extension of PCa within the specimen was transferred to a schematic diagram, according to Bettendorf et al. *(13)* and Eminaga et al. *(17)*. The PCa-map consists of 22 segments including 2 segments for the seminal vesicles. The digitized data was the basis of the calculation of the percentage of the tumor volume. The Gleason Score of each segment was individually documented. An example of a PCA-mapis depicted in Figure 1.

Statistical analysis

SPSS Statistics 23 (IBM) was used for analysis. Sensitivity, specificity, positive predictive value, negative predictive value, positive and negative likelihood ratios were calculated for all available segments. A Kruskal-Wallis-Test was performed to compare the SUVmax median of true positive and true negative segments. We estimated the diagnostic performance of PSMA-PET by calculating the area under the receiver operator characteristic curve (ROC-AUC). Two-sided p-values <0.05 were considered

statistically significant.

Results

Histological results of 132 segments in six patients were available. Two segments of each patient were excluded from the analysis since they could not be identified in PET because of failing assignment to imaging. In two patients (# 2 and 5) four segments adjacent to the bladder were excluded because of spillover of urine activity. Thus, a total of 112 segments were included in the statistical analysis.

Detailed clinical data and histopathological results of the patients are summarized in Table 1.

Comparison of PCa-maps, Gleason Scores and PSMA-PET -imaging

Only 3 of 37 segments without histological PCa on the PCa-maps were considered as positive on the corresponding slices in PSMA-PET, resulting in a specificity of 92% (Table 2). Defining the PCa-maps as gold-standard, the sensitivity of PSMA-PET for the identification of areas with PCa was 92%. Within the 3 false positive segments one showed a active prostatitis, one a chronic prostatitis and one presented a high grade prostatic intraepithelial neoplasia (PIN).

The positive and negative likelihood ratio for PSMA-PET detecting PCa were 11.5 and 0.09, respectively. The positive and negative predictive values were 96% and 85%, respectively, indicating a strong and exact correlation of PSMA positivity with the actual histological presence of prostate cancer within the prostatic gland. The SUVmax within the true positive segments was significantly higher than in true negative prostate segments (median, 11.0±7.8 vs. 2.7±0.9, p<0.001, Kruskal-Wallis-Test).

A ROC-AUC analysis of SUVmax values (Figure 2) in correlation with the histologic results revealed an AUC of 0.93 (95% confidence interval: 0.89 – 0.99, p < 0.001). Using a SUVmax cutoff of 4.0, a sensitivity and specificity of 88% and 86.5%, and an accuracy of 87.5% were achieved.

Comparing Gleason scores and ^{68}Ga-PSMA-PET results (Figure 3) showed a high detection rate of true positive segments even in lower Gleason scores of 3+3=6 with 80% true positive segments.

The Box-Plot of the SUVmax values allotted to the distribution of the Gleason Scores shows a tendency of increasing the SUVmax values, but because of the small number of patients, no statistical analysis was performed (Figure 3).

Discussion

Preoperative information on localization and extent of PCa within the prostate is limited and still lacks accuracy and could result in inappropriate treatment *(18)*. Multiparametric magnetic resonance imaging (mp-MRI) is increasingly used to display the local tumor burden within the prostate. However, despite its ability to detect PCa lesions with a Gleason Score of ≥7, especially in larger tumor foci it has clinically significant limitations in smaller lesions and lesions with a Gleason Score of <7. In a study on mp-MRI used prior to RPE and correlated with the true tumor extent Le et al. found that 80 % of tumors were detected. However, smaller tumors with a diameter of less than 1 cm were missed by mp-MRI in the majority of cases, even in some cases of high grade lesions. Lesions with a Gleason score of 6 were missed in 80% of cases independent of the diameter of the lesions *(19)*.

In contrast, PSMA-PET-imaging has reliable specificity and sensitivity in PCa even when

Gleason Score is 6 or less (9). The present preliminary analysis compares the preoperative PSMA-PET/CT imaging with postoperative PCa-maps of the prostate. The results indicate high accuracy in prediction of the pattern of cancer growth in the prostate by regional PSMA-uptake.

To date there are only two recent publications reporting of PSMA uptake in the prostate prior to RPE (20, 21). Budäus et al. report only about ^{68}Ga-PSMA enabling visualization of PCa in the prostate gland (20). Using a 12 segment model Rowe et al. showed a poor sensitivity of 10% and an accuracy of 56% in detection of malignant lesions in the prostate in the stringent analysis using a ^{18}F-labled PSMA tracer (^{18}F-DCBC), which has a lower tumor to background contrast and seems to have a low capability compared to ^{68}Ga-PSMA- HBED-CC (21). In the same patient cohort mp-MRI resulted in a sensitivity of 35% and an accuracy of 62% in the stringent analysis. In contrast, applying PSMA-PET-imaging, our results show a high sensitivity of 92% and an accuracy of 92% in detecting malignant lesions using a 22 segment model of the prostate. In addition to the superior tumor to background contrast of ^{68}Ga-PSMA- HBED-CC, this discrepancy might be explained by the fact that in the present study PSMA-PET/CT images were reangulated concordant to prostate histology workup in which the prostate is sliced axial to the urethra. A curved reangulation might even better match the prostate histology slices and should be evaluated in further studies.

Furthermore our results indicate a significantly higher tumor uptake in the malignant lesions compared to the PCa free segments (median SUVmax, 11.0±7.8 vs. 2.7±0.9, $p<0.001$) which is in line with the results of Rowe et al., however, their study lower SUVmax values using ^{18}F-labled PSMA tracer (median SUVmax, 3.5 vs. 2.2; p = 0.004).

In the present study we thoroughly correlated histopathological findings with PSMA-PET information and could confirm results published by Afshar-Oromieh et al. who recently found that ^{68}Ga-PSMA- HBED-CC can also be used to reliably detect PCa with low Gleason scores ≤ 7 *(9)*.

Recent publications have demonstrated increasing importance of PSMA imaging in patients with prostate cancer according to local recurrence or metastatic disease (9, 12, 21). Considering patients for PSMA imaging to rule out metastatic disease prior prostatectomy must be done with caution to patient history of other disease and potential PSMA positive pitfalls must be considered in image analysis. Recent studies and case reports have shown high ^{68}Ga-PSMA uptake e.g. in schwannomas, coeliac ganglia and even differentiated thyroid cancer (22-24). The presence of metastases changes therapy options significantly.

Our study is limited by deficiencies inherent to a retrospective approach and the small number of patients. To avoid spillover from urine activity in the bladder an indwelling catheter to empty the bladder prior imaging could be used. Despite these limitations, the present findings are a strong hint that cross section imaging supported by PSMA-PET information may be helpful for understanding the localization and extent of PCa within the prostate prior to both biopsy and definitive therapy.

Particularly, this novel technique could have the potential to significantly improve decision making concerning the selection of the optimal definitive PCa therapy for individual patients. If our results could be confirmed in larger collectives PSMA-PET imaging could help to select patients to focal or radical treatment, and in case of radical

prostatectomy, to a nerve sparing approach versus an RPE with wide excision of the prostate.

Currently, the data presented here are being validated; optimizing imaging protocols e.g. dynamic acquisition or dual-time imaging seems to even provide a higher contrast of PSMA-activity and further improve sensitivity.

Conclusions

This preliminary proof of concept study shows that the intraprostatic localization and extent of PCa may be estimated by PSMA-PET technology with high accuracy. Therefore, this imaging method may be helpful for identifying target lesions prior to prostate biopsy and may support decision-making prior to focal or radical PCa therapy. Larger studies with dedicated imaging protocols are needed to evaluate the significance of these data, especially in use of hybrid imaging systems, such as PET/MRI.

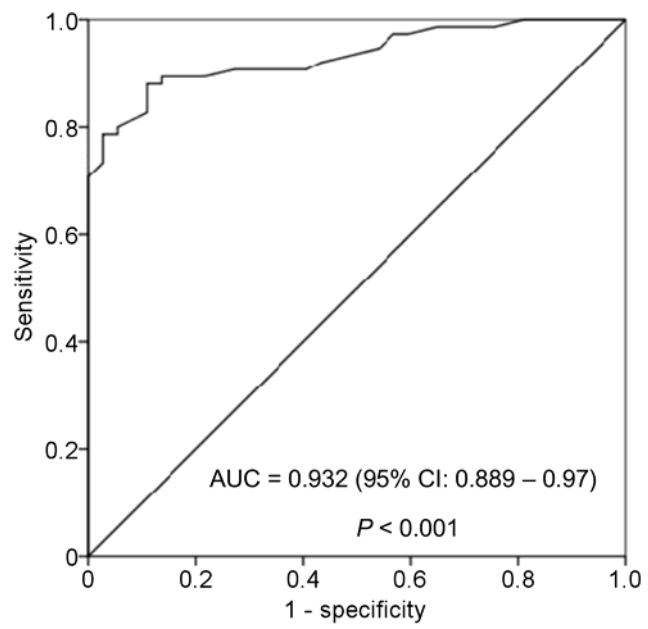## Acknowledgement

Conflict of Interest
The authors declare they have no conflict of interest according to the subject and matter presented in the study.

References

1. Siegel RL, Miller KD, Jemal A. Cancer statistics, 2015. *CA Cancer J Clin*. 2015;65:5-29.

2. Etzioni R, Gulati R, Mallinger L, Mandelblatt J. Influence of study features and methods on overdiagnosis estimates in breast and prostate cancer screening. *Ann Intern Med*. 2013;158:831-838.

3. Wilt TJ, Brawer MK, Barry MJ, et al. The Prostate cancer Intervention Versus Observation Trial:VA/NCI/AHRQ Cooperative Studies Program #407 (PIVOT): design and baseline results of a randomized controlled trial comparing radical prostatectomy to watchful waiting for men with clinically localized prostate cancer. *Contemp Clin Trials*. 2009;30:81-87.

4. Davis MI, Bennett MJ, Thomas LM, Bjorkman PJ. Crystal structure of prostate-specific membrane antigen, a tumor marker and peptidase. *Proc Natl Acad Sci U S A*. 2005;102:5981-5986.

5. Wright GL, Jr., Grob BM, Haley C, et al. Upregulation of prostate-specific membrane antigen after androgen-deprivation therapy. *Urology*. 1996;48:326-334.

6. Ross JS, Sheehan CE, Fisher HA, et al. Correlation of primary tumor prostate-specific membrane antigen expression with disease recurrence in prostate cancer. *Clin Cancer Res*. 2003;9:6357-6362.

7. Troyer JK, Beckett ML, Wright GL, Jr. Detection and characterization of the prostate-specific membrane antigen (PSMA) in tissue extracts and body fluids. *Int J Cancer*. 1995;62:552-558.

8. Sokoloff RL, Norton KC, Gasior CL, Marker KM, Grauer LS. A dual-monoclonal sandwich assay for prostate-specific membrane antigen: levels in tissues, seminal fluid and urine. *Prostate*. 2000;43:150-157.

9. Afshar-Oromieh A, Avtzi E, Giesel FL, et al. The diagnostic value of PET/CT imaging with the (68)Ga-labelled PSMA ligand HBED-CC in the diagnosis of recurrent prostate cancer. *Eur J Nucl Med Mol Imaging*. 2015;42:197-209.

10. Heidenreich A, Pfister D, Porres D. Cytoreductive radical prostatectomy in patients with prostate cancer and low volume skeletal metastases: results of a feasibility and case-control study. *J Urol*. 2015;193:832-838.

11. Neugut AL, Gelmann EP. Treatment of the Prostate in the Presence of Metastases: Lessons from Other Solid Tumors. *Eur Urol*. 2015;doi:10.1016/j.eururo.2015.06.004 [Epub ahead of print]

12. Afshar-Oromieh A, Haberkorn U, Eder M, Eisenhut M, Zechmann CM. [68Ga]Gallium-labelled PSMA ligand as superior PET tracer for the diagnosis of prostate cancer: comparison with 18F-FECH. *Eur J Nucl Med Mol Imaging*. 2012;39:1085-1086.

13. Bettendorf O, Oberpenning F, Kopke T, et al. Implementation of a map in radical prostatectomy specimen allows visual estimation of tumor volume. *Eur J Surg Oncol*. 2007;33:352-357.

14. Association of Clinical P. Guidelines for the macroscopic processing of radical prostatectomy and pelvic lymphadenectomy specimens. *J Clin Pathol*. 2008;61:713-721.

15. Epstein JI, Allsbrook WC, Jr., Amin MB, Egevad LL. Update on the Gleason grading system for prostate cancer: results of an international consensus conference of urologic pathologists. *Adv Anat Pathol*. 2006;13:57-59.

16. Sobin LH, Gospodarowicz MK, Wittekind C. International Union against Cancer. TNM classification of malignant tumours. 7th ed. *Chichester, West Sussex, UK; Hoboken, NJ.* 2010;Wiley-Blackwell.

17. Eminaga O, Hinkelammert R, Semjonow A, et al. Clinical map document based on XML (cMDX): document architecture with mapping feature for reporting and analysing prostate cancer in radical prostatectomy specimens. *BMC Med Inform Decis Mak*. 2010;10:71.

18. Busch J, Magheli A, Leva N, et al. Higher rates of upgrading and upstaging in older patients undergoing radical prostatectomy and qualifying for active surveillance. *BJU Int*. 2014;114:517-521.

19. Le JD, Tan N, Shkolyar E, Lu DY, Kwan L, Marks LS et al. Multifocality and prostate cancer detection by multiparametric magnetic resonance imaging: correlation with whole-mount histopathology. *Eur Urol*. 2015;67:569-576.

20. Budaus L, Leyh-Bannurah SR, Salomon G, et al. Initial Experience of Ga-PSMA PET/CT Imaging in High-risk Prostate Cancer Patients Prior to Radical Prostatectomy. *Eur Urol*. 2015. doi:10.1016/j.eururo.2015.06.010.

21. Rowe SP, Gage KL, Faraj SF, et al.: 18F-DCFBC PET/CT for PSMA-Based Detection and Characterization of Primary Prostate Cancer. *J Nucl Med*, 2015;56:1003-10.

22. Ripschler C, Maurer T, Schwaiger M, Eiber M. Intense PSMA-expression using 68Ga-PSMA PET/CT in a paravertebral schwannoma mimicking prostate cancer metastasis. Eur J Nucl Med Mol Imaging 2015 Oct 27. [Epub ahead of print]

23. Krohn T, Verburg FA, Pufe T et al.: 68Ga-PSMA-HBED uptake mimicking lymph node metastasis in cloeliac ganglia: an important pitfall in clinical practice. Eur J Nucl Med Mol Imaging, 2015;42:210-214.

24. Verburg FA, Krohn T, Heinzel A, Mottaghy FM, Behrendt FF. First evidence of PSMA expression in differentiated thyroid cancer using 68Ga-PSMA-HBED-CC PET/CT. Eur J Nucl Med Imaging, 2015:1622-1623.

Figure 1.

Reangulated slices show concordance of PSMA distribution and histology maps of patient 1. Arrows show PSMA uptake in the seminal vesicles. "10" represents a 10 mm positive surgical margin.

Figure 2.

ROC-AUC Curve of SUVmax according to histological results. AUC = Area Under the Curve, CI: Confidence Interval
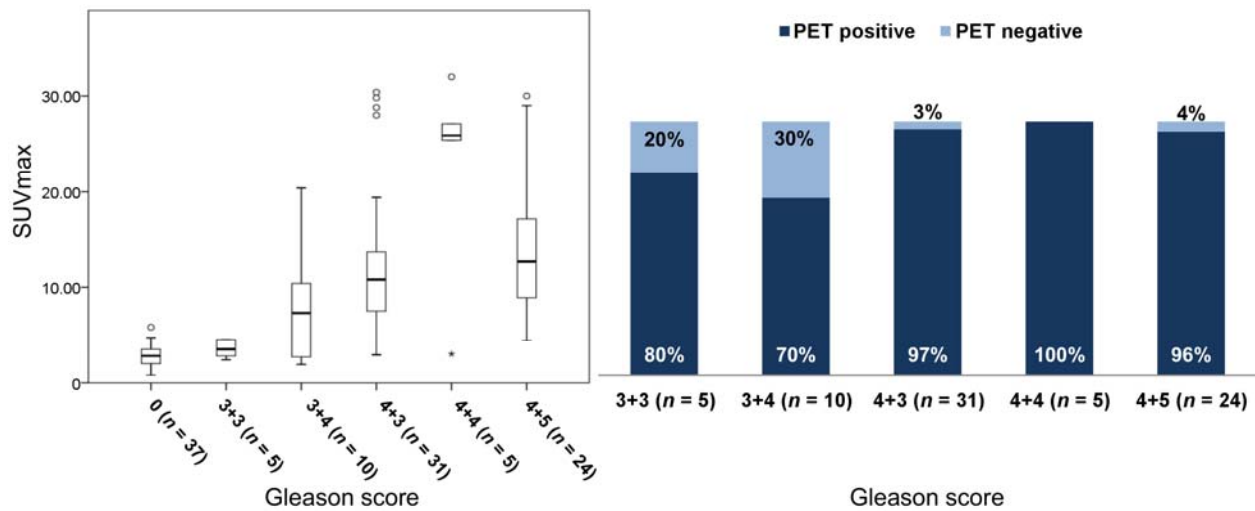
Figure 3.

On the left side the SUVmax values are plotted according to different loco regional Gleason Scores. On the right side respective true positive segments detection rates using ^{68}Ga-PSMA-PET are depicted. SUVmax = Maximum Standard Uptake Value; PET = Positron Emission Tomographie

Table 1: Pre- and postoperative characteristics of studied patients with prostate cancer.

	Patient 1	Patient 2	Patient 3	Patient 4	Patient 5	Patient 6
Prostate Biopsy						
Age [years]	59	57	73	72	73	56
iPSA [ng/ml]	111.1	5.7	27.0	30.6	9.6	76.3
Gleason Score pBx	4+3=7b	3+4=7a	3+4=7a	4+3=7b	3+4=7a	8
Location PCa	Bilateral Left > right	Bilateral Right > left	Bilateral Equally distributed	Unilateral Left	Bilateral Right > left	Bilateral Equally distributed
Number of positive cores	6/10	5/8	5/6	3/12	7/10	11/11
Clinical stage	cT2c (left lobe)	cT2a (Right base)	cT1	cT1	cT2c (bilateral)	cT2c (both lobes)
TRUS suspicious of PCa **TRUS Prostate volume [cm³]**	Left lobe 36	Right base 40	Normal 36	Normal 39	Right base 17	Both lobes 49
Staging						
Bone Scan (Indication) **Result**	Not Done (PSMA-PET)	Routine Scan *Lesion Os ilium left*	PSA-Elevation *Exclusion of Mets*	Not Done (PSMA-PET)	Routine Scan *Lesion Lumbar vertebra III*	Not Done (PSMA-PET)
PSMA-PET-CT (Indication) **Result**	Exclusion of Metastasis Parailiacal Lnn. Metastases	Suspicious lesion in Bone scan Equivocal bony lesion	Exclusion of Metastasis No lesions	Exclusion of Metastasis No lesions	Exclusion of Metastasis No lesions	Exclusion of Metastasis Iliacal, aortal, pararectal Lnn. Metastases
Radical Prostatectomy						
Prostate volume [cm³] **PCa volume [cm³] (%)**	48 20.9 (43.5)	34 2.6 (7.8)	40 5.7 (14.6)	52 14.5 (27.9)	30 7.8 (26.5)	51 30.2 (59.2)
Gleason Score	4+3=7b	3+4=7a	4+3=7b	4+3=7b	4+5=9a	4+5=9a
Positive surgical margin	Yes (left apex)	No	Yes (right anterior)	Yes (left seminal vesicle)	No	Yes (left posterior)
Invasion of seminal vesicles	Yes (both)	Yes (left)	No	Yes (left)	Yes (both)	Yes (both)
Pathological stage	pT3b pN1	pT3b pN0	pT3a pN0	pT3b pN1	pT3b pN0	pT3b N1

Abbreviations: iPSA = initial prostate specific antigen; pBx = prostate biopsy; PCa = prostate carcinoma; TRUS = transrectal ultrasound; PSMA-PET-CT = prostate specific membrane antigen positrone tomography computer tomography, Lnn.= lymphonodal

Table 2:

Results of ^{68}Ga-PSMA-PET of the prostate segments verified by histopathology after RPE.

	Histology positive n = 75, n	Histology negative n = 37, n (95% CI)	
PSMA positive n = 72	69	3	PPV 96%
PSMA negative n = 40	6	34	NPV 85%
	Sensitivity (95% CI) 92% (0.83 - 0.97)	Specificity (95 % CI) 92% (0.77 - 0.98)	Accuracy 92%
PPV = positive predictive value; NPV = negative predictive value; PSMA = prostate-specific membrane antigen; CI = Confidence Interval			